Synthesis, Spectral Stability, and Electroluminescent Properties of Random Poly(2,7-fluorenylenevinylene-*co*-3,6-carbazolylenevinylene) Obtained by a Suzuki−Heck Cascade Reaction

Roberto Grisorio,[†] Piero Mastrorilli,[†] Cosimo F. Nobile,*[,†] Giuseppe Romanazzi,[†] Gian P. Suranna,[†] Giuseppe Gigli,[‡,§] Claudia Piliego,[‡,○] Giuseppe Ciccarella,[§] Pynalisa Cosma,[||] Domenico Acierno,[#] and Eugenio Amendola[⊗]

Department of Water Engineering and Chemistry (DIAC), Polytechnic of Bari, Via Orabona 4, I-70125 Bari, Italy, National Nanotechnology Laboratories (NNL) of CNR-INFM Via Arnesano, 73100 Lecce, Italy, Istituto Superiore Universitario di Formazione Interdisciplinare (ISUFI)-sezione Nanoscienze, Via Arnesano, 73100 Lecce, Italy, Dipartimento di Ingegneria dell' Innovazione, University of Lecce, Via Monteroni, I-73100, Lecce, Italy, Department of Chemistry, University of Bari, Via Orabona 4, I-70125 Bari, Italy, Department of Materials and Production Engineering (DIMP), University of Naples Federico II, p.le Tecchio 80, I-80125 Naples, Italy, and Institute of Composite and Biomedical Materials (IMCB), Italy's National Research Council, p.le Tecchio 80, I-80125 Naples, Italy

Received January 26, 2007; Revised Manuscript Received April 17, 2007

ABSTRACT: The synthesis of a series of new random poly(9,9-dioctyl-2,7-fluorenylenevinylene-*co*-*N*-octyl-3,6-carbazolylenevinylene) copolymers at 20−80% mol/mol of carbazole (**P2**−**P6**) was achieved by a versatile Suzuki−Heck reaction cascade between the suitable dibromoaryl derivatives at different monomer ratios and potassium vinyltrifluoroborate. Their properties have been investigated by ^{1}H NMR, IR, TGA, DSC, cyclic voltammetry, UV−vis, and photoluminescence and compared to those of poly(9,9-dioctyl-2,7-fluorenylenevinylene) (**P1**) obtained by the same method. The control of the π-conjugation extension and the inductive effects, determined by the amount of carbazolyl-3,6-ene moieties, permitted the modulation of the HOMO and LUMO energy levels of these materials without remarkably modifying their emission properties. Furthermore, different from poly(9,9-dioctylfluorene), a good spectral stability in the solid state was proven for **P1** after a thermal annealing under air at 130 °C. The electroluminescence properties of the materials were tested by constructing OLED devices of ITO/PEDOT−PSS/**P1**−**P6**/Ca/Al configuration. The improvement of the device performances for **P2**−**P4** (20−50 mol/mol of carbazole) with respect to **P1** was attributed to the better hole transport in the material because of the presence of carbazole units. The better performances of **P5** (450 cd/m^2 at 22 V, 0.0225 cd/A at 22 V) were ascribed to the easier injection of electrons in the device with respect to the other copolymers, as a consequence of its higher electron affinity. These figures of merit could be improved by inserting a suitable electron injecting layer (Alq_3) between the cathode and **P5** (890 cd/m^2 at 18 V, 0.0435 cd/A at 10 V).

Introduction

The discovery of electroluminescence from organic π-conjugated materials has boosted an enormous research interest in the field of fluorescent π-conjugated polymers as active layers for organic light emitting diodes (OLEDs).[1] Considerable efforts have been devoted to the chemical modification of polymer structures by the introduction of different functional groups on their π-conjugated backbone or by copolymerization between suitable moieties. The chemical modification of a π-conjugated system can affect its physical properties by two contributions: (i) an inductive effect exerted by the introduction of specific functional groups on the polymer backbone and (ii) the degree of the π-conjugation extension, which can be influenced not only by the length of the conjugated segment, but also by the type of the chemical bonds involved in the conjugation (aryl moieties, double or triple bonds) as well as by conformational aspects. All these contributions can independently influence the HOMO and LUMO energy levels of a π-conjugated system.[2] The great variety of the synthesizable π-conjugated backbones and of synthetic approaches easily allows the fine-tuning of the emitted color of the organic materials and can favor the injection of holes and electrons in devices by adjusting their HOMO and LUMO energy levels,[3] a degree of freedom unattainable with inorganic semiconductors.

The choice of potential materials for application in OLEDs, however, has to be restrained to highly fluorescent systems, which is an intrinsic prerequisite for good performances in devices. Among these, polyfluorenes (PFs) are the most investigated blue-emitting materials, due to their unique photoluminescence efficiency in the solid state and the easy functionalization of the C-9 position of fluorene, which permits to control the solubility as well as the interchain interactions in the solid state of the corresponding macromolecules.[4] However, the potentialities of PFs as active layers in OLEDs are still limited by their poor spectral stability, because of the appearance, in the course of device operation, of a green emission band, consequence of the fluorene C-9 oxidation.[5] The physical reasons of such poor spectral stability are still debated and have been assigned to on-chain fluorenone[6] or fluorenone-induced excimer[7] emission. The design of suitable polymer structures is therefore crucial in order to stabilize the optical properties of fluorene-based materials. Poly(fluorenylenevinylene)s (PFVs,

* Corresponding author. E-mail: nobile@poliba.it. Telephone: +390805963666. Fax: +390805963611.
[†] Department of Water Engineering and Chemistry (DIAC), Polytechnic of Bari.
[‡] National Nanotechnology Laboratories (NNL) of CNR-INFM.
[§] Dipartimento di Ingegneria dell' Innovazione, University of Lecce.
[||] Department of Chemistry, University of Bari.
[#] Department of Materials and Production Engineering (DIMP), University of Naples Federico II.
[⊗] Institute of Composite and Biomedical Materials (IMCB), Italy's National Research Council.
[○] ISUFI-sezione Nanoscienze.

10.1021/ma070221q CCC: $37.00
Published on Web 06/09/2007

Chart 1

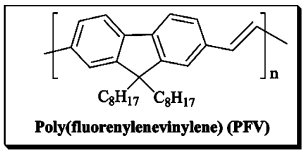

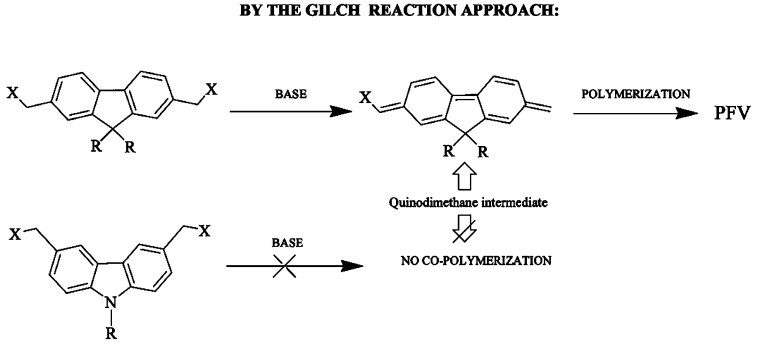

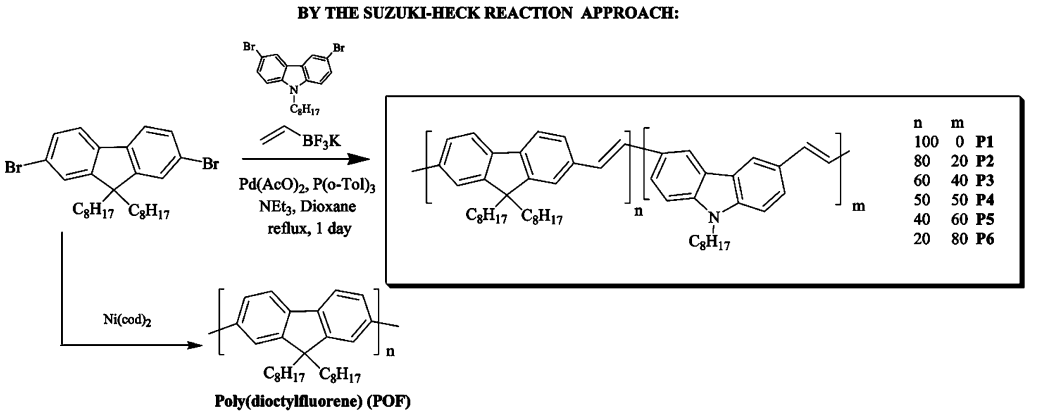

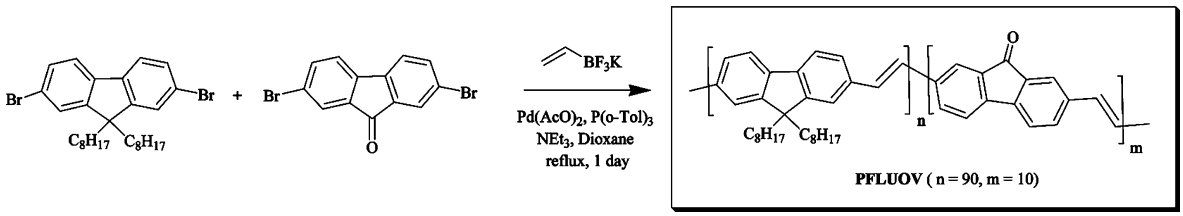

Chart 1) represent an attractive class of fluorescent materials[8−11] and, differently from PFs, are characterized by the presence of double bonds linking two fluorenylene systems, shifting the emission of PFVs to the blue-green region.

The obtainment of PFVs is commonly pursued by three major synthetic strategies: the Wittig condensation,[8] the Heck reaction,[9] and the widely preferred Gilch route.[10] Concerning the preparation of random fluorenylenevinylene copolymers, the properties of which have stimulated the interest of various research groups, as confirmed by a very recent work of Jin et al.,[12] the Gilch approach is the most versatile, because the Wittig condensation and the Heck reaction are mostly employed for synthesis of alternating PFVs copolymers. In this framework, we have recently proposed a versatile method for the obtainment of random PFVs by a one-pot Suzuki−Heck cascade reaction using potassium vinyltrifluoroborate as ethylene equivalent,[13] and the suitable aryl dibromides. Compared to other synthetic approaches, this protocol envisages the use of aryl dibromides, which are simple and readily available building blocks for the preparation of functionalized random polyarylenevinylenes (PAVs). In particular, the Gilch approach is useless for the synthesis of target PFV containing 3,6-carbazole as comonomer, since 3,6-dihalomethyl carbazole cannot give the quinodimethane intermediate required for the propagation step of the reaction[14] (Chart 1).

Here, we describe the synthesis and properties of new random PFVs containing 3,6-*N*-octylcarbazole at various compositions. Our interest toward 3,6-carbazole containing PAVs is motivated by the strong hole-transporting ability of such systems in optoelectronic devices (due to the electron-donating properties of the nitrogen atom) and by the 3,6 linkage at the carbazole moiety, which determines the interruption of the π-conjugation extension.[15] We investigated the possibility to modify the HOMO and LUMO energy levels of PFV segments without changing their emission properties. This aim was pursued by modulating the ionization potential and electron affinity of random poly(9,9-dioctyl-2,7-fluorenylenevinylene-*co*-*N*-octyl-3,6-carbazolylenevinylene) through variation of the amount of carbazole in the random PFVs.

Experimental Section

All manipulations were carried out under inert nitrogen atmosphere using Schlenk techniques. All solvents were carefully dried and freshly distilled prior to use. 2,7-Dibromofluorene, 3,6-dibromocarbazole, palladium(II) acetate, tri(*o*-tolyl)phosphane and all other reactants were purchased from Aldrich, Acros or Fluka and used without further purifications. NMR spectra were recorded at 295 K on a Bruker Avance 400 MHz. UV−vis spectra were recorded on a Kontron Uvikon 942 instrument and fluorescence spectra were obtained on a Varian Cary Eclipse spectrofluorimeter. FT-IR measurements were recorded on a Bruker Vector 22 spectrophotometer. Gel permeation chromatography (GPC) analyses were carried out on an Agilent Series 1100 instrument equipped with a Pl-gel 5 μm mixed-C column. THF solutions for GPC analysis were eluted at 25 °C at a flow rate of 1.0 mL/min and analyzed using a multiple wave detector. Molecular weights and molecular weight distributions are relative to polystyrene. Thermogravimetric analyses (TGA) were carried out with a thermobalance TA Instruments 2590; differential scanning calorimetry (DSC) was measured on a TA Instruments 2920 calorimeter. All thermal analyses were carried out under nitrogen flow with a heating rate of 10 °C/min. Cyclic voltammetry measurements were carried out under inert nitrogen atmosphere with an Autolab potentiostat PGSTAT 10 using a three-electrode cell. The CV measurements were carried out in acetonitrile solutions of tetrabutylammonium tetrafluoroborate (0.10 M) at a scan rate of 100 mV/s under nitrogen. An indium−tin oxide (ITO) electrode coated with a thin film of the relevant polymer was used as the working electrode. A Pt wire and a $Ag/AgNO_3$ electrode were utilized as the counter electrode and reference electrode respectively. All measurements were calibrated against ferrocene, the ionization potential of which is −4.80 eV. The evaluation of the HOMO level of the polymers was carried out by measuring the onset of the oxidation potential in the anodic scan. The OLED devices were prepared by spin-coating the hole transporting layer, namely poly(3,4-ethylenedioxythiophene) (PEDOT-PSS) onto an O_2-plasma treated ITO coated glass substrate. Subsequently, the active material was spin-cast from a chloroform solution (2 mg in 0.3 mL $CHCl_3$) and finally a calcium (45 nm) /aluminum (150 nm) electrode was deposited by thermal evaporation (10^{-6} mbar). In the case of the optimized device, a 5 nm layer of Alq_3 was thermally evaporated before Ca/Al deposition. The characterization of the devices was performed at RT in air.

2,7-Dibromo-9,9-dioctylfluorene.[16] A mixture of 2,7-dibromofluorene (2.500 g, 7.71 mmol) and tetrabutylammonium bromide (0.795 g, 2.46 mmol) in a 50% w/v NaOH aqueous solution (16 mL) was stirred for 15 min at 60 °C. To the red suspension was added 1-bromooctane (3.027 g, 15.40 mmol), and the mixture was kept under stirring overnight. After the solution had cooled, the product was extracted with diethyl ether and the organic layer dried over Na_2SO_4. After removing the solvent, the crude was purified by flash chromatography (SiO_2, petroleum ether 40−60 °C) to afford 2,7-dibromo-9,9-dioctylfluorene in 85% yield as white solid. Mp = 52.3−52.8 °C. ^{1}H NMR (400 MHz, $CDCl_3$): δ 7.50 (dd, J = 7.5, 1.3 Hz, 2H), 7.47 (d, J = 1.8 Hz, 2H), 7.45 (d, J = 1.3 Hz, 2H), 1.91−1.95 (m, 4H), 1.05−1.26 (m, 20H), 0.83 (t, J = 7.6 Hz, 6H), 0.52−0.62 (m, 4H). ^{13}C NMR (100 MHz, $CDCl_3$): δ 152.4, 139.0, 130.2, 126.1, 121.4, 120.8, 55.4, 40.1, 31.8, 29.9, 29.2, 29.1, 23.7, 22.7, 14.2.

2,7-Dibromofluoren-9-one. To a solution of 2,7-dibromofluorene (5.000 g, 15.43 mmol) in acetic anhydride (70 mL) was slowly added CrO_3 (3.750 g, 37.50 mmol) at 0 °C. After 2 h of stirring, the solution was allowed to reach room temperature and reacted overnight. After the solvent was removed, the crude product was purified by flash chromatography (SiO_2, petroleum ether 40−60 °C/CH_2Cl_2 = 6/1) and subsequent crystallization from isopropanol to afford 2,7-dibromofluoren-9-one in 70% yield as a yellow solid. Mp = 205.0−205.5 °C. ^{1}H NMR (400 MHz, $CDCl_3$): δ 7.76 (d, J = 1.8 Hz, 2H), 7.63 (dd, J = 7.9, 1.8 Hz, 2H), 7.38 (d, J = 7.9 Hz, 2H). ^{13}C NMR (100 MHz, $CDCl_3$): δ 191.2, 142.3, 137.5, 135.3, 127.9, 123.4, 121.9.

3,6-Dibromo-*N*-octylcarbazole. To a mixture of 3,6-dibromocarbazole (1.295 g, 4.01 mmol) in DMSO (8 mL) and a 50% w/v NaOH aqueous solution (4 mL) was added 1-bromooctane (1.150 g, 5.97 mmol) in one portion. The resulting solution was vigorously stirred for 6 h at room temperature. Then the organic phase was extracted with diethyl ether, washed with brine and dried over Na_2SO_4. After the solvent was removed, the crude product was purified by flash cromatography (SiO_2, petroleum ether 40−60 °C) to afford 3,6-dibromo-*N*-octylcarbazole in 84% yield as a white solid. Mp = 86.7 − 88.6 °C. ^{1}H NMR (400 MHz, $CDCl_3$): δ 8.11 (d, J = 1.8 Hz, 2H), 7.55 (dd, J = 8.5, 1.8 Hz, 2H), 7.24 (d, J = 8.5 Hz, 2H), 4.19 (t, J = 6.7 Hz, 2H), 1.85−1.77 (m, 2H), 1.39−1.19 (m, 10H), 0.89 (t, J = 6.7 Hz, 3H). ^{13}C NMR (100 MHz, $CDCl_3$): δ 139.3, 129.0, 123.4, 123.2, 127.9, 111.9, 110.4, 43.3, 31.8, 29.3, 29.2, 28.9, 27.3, 22.6, 14.1.

Potassium Vinyltrifluoroborate. The synthesis of this compound was carried out by slightly adapting a literature procedure.[17] To a solution of trimethyl borate (20.78 g, 0.20 mol) in THF (100 mL) was added 100 mL of a vinylmagnesium chloride solution in THF (1.6 M, 0.16 mol) at −80 °C. The mixture was allowed to reach room temperature and was stirred for 1 h. Subsequently, KHF_2 (61.70 g, 0.79 mol) was added to the solution at 0 °C followed by slow addition of water (100 mL). The resulting solution was reacted at room temperature for 1 h, and eventually the solvent was removed. The crude product was extracted with acetone in a Soxhlet apparatus to afford potassium vinyltrifluoroborate in 85% yield as a white solid. ^{1}H NMR (400 MHz, $CDCl_3$): δ 5.93−5.77 (m, 1H), 5.31 (dd, J = 19.5, 4.3 Hz, 1H), 5.18 (d, J = 10.4 Hz, 1H). ^{13}C NMR (100 MHz, $CDCl_3$): δ 120.1 (q, $^3J_{C,F}$ = 4.6 Hz).

Poly(9,9-dioctyl-2,7-fluorenylenevinylene) (P1). A solution of 2,7-dibromo-9,9-dioctylfluorene (0.548 g, 1.00 mmol), potassium vinyltrifluoroborate (0.147 g, 1.10 mmol), $Pd(AcO)_2$ (11.0 mg, 0.05 mmol), P(*o*-Tol)$_3$ (0.076 g, 0.25 mmol), triethylamine (0.35 mL, 2.5 mmol) in dioxane (5 mL) was refluxed for 1 day. After cooling to room temperature, the solution was poured into methanol (100 mL). The obtained solid was filtered and dissolved in the minimum amount of chloroform for reprecipitation in methanol. Then, the polymer was washed with acetone in a Soxhlet apparatus and extracted with chloroform to give **P1** in 80% yield as a green powder. Anal. Calcd: C, 89.79; H, 10.21. Found: C, 87.24; H, 9,87. ^{1}H NMR (400 MHz, $CDCl_3$): δ 7.88−7.16 (m, aromatic and vinyl protons, 8H), 2.29−1.79 (m, 4H), 1.40−0.94 (m, 20H), 0.93−0.49 (m, 10H). IR (KBr): ν [cm^{-1}] 3020, 2975, 2931, 2868, 1598, 1464, 1356, 957 (*trans*-HC═CH), 817, 734.

Poly(9,9-dioctyl-2,7-fluorenylenevinylene-*co*-*N*-octyl-3,6-carbazolylenevinylene) (P4). A solution of 2,7-dibromo-9,9-dioctylfluorene (0.274 g, 0.50 mmol), 3,6-dibromo-*N*-octylcarbazole (0.217 g, 0.50 mmol), potassium vinyl-trifluoroborate (0.147 g, 1.10 mmol), $Pd(AcO)_2$ (11.0 mg, 0.05 mmol), P(*o*-Tol)$_3$ (0.076 g, 0.25 mmol), and triethylamine (0.35 mL, 2.5 mmol) in dioxane (5 mL) was refluxed for 1 day. After cooling to room temperature, the solution was poured into methanol (100 mL). The obtained solid was filtered and dissolved in the minimum amount of chloroform for reprecipitation in methanol. Then, the polymer was washed with acetone in a Soxhlet apparatus and extracted with chloroform to give **P4** in 91% yield as a green powder. Anal. Calcd: C, 88.65; H, 9.40; N, 1.95. Found: C, 86.09; H, 9.50; N, 1.88. ^{1}H NMR (400 MHz, $CDCl_3$): δ 8.43−8.12 (m, 2H), 7.82−7.09 (m, aromatic and vinyl protons, 14H), 4.44−4.19 (m, 2H), 2.19−1.80 (m, 6H), 1.47−0.98 (m, 30H), 0.94−0.60 (m, 13H). IR (KBr): ν [cm^{-1}] 3026, 2953, 2933, 2857, 1587, 1490, 1463, 1346, 1085, 962 (*trans*-HC═CH), 797, 686.

The other carbazole containing copolymers comprising carbazole were prepared analogously. **P2**: yield 79%, green powder. Anal. Calcd: C, 89.37; H, 9.91; N, 0.71. Found: C, 86.40; H, 10.28; N, 0.80. ^{1}H NMR (400 MHz, $CDCl_3$): δ 8.43−8.12 (m, 0.5H), 7.82−7.09 (m, aromatic and vinyl protons, 11.0H), 4.44−4.19 (m, 0.5H), 2.19−1.80 (m, 4.5H), 1.47−0.98 (m, 25.0H), 0.94−0.60 (m, 11.5H). IR (KBr): ν [cm^{-1}] 3029, 2954, 2933, 2858, 1587, 1490, 1463, 1346, 1085, 962 (*trans*-HC═CH), 797, 686. **P3**: yield 87%, green powder. Anal. Calcd: C, 88.90; H, 9.58; N, 1.51. Found: C, 85.44;

H, 9.92; N, 1.52. ^{1}H NMR (400 MHz, $CDCl_3$): δ 8.43−8.12 (m, 1.4H), 7.82−7.09 (m, aromatic and vinyl protons, 12.2H), 4.44−4.19 (m, 1.4H), 2.19−1.80 (m, 5.4H), 1.47−0.98 (m, 27.0H), 0.94−0.60 (m, 12.1H). IR (KBr): ν [cm^{-1}] 3025, 2929, 2868, 1598, 1464, 1356, 959 (*trans*-HC═CH), 817, 734. **P5**: yield 92%, green powder. Anal. Calcd: C, 88.37; H, 9.21; N, 2.42. Found: C, 85.59; H, 9.60; N, 2.45. ^{1}H NMR (400 MHz, $CDCl_3$): δ 8.44−8.13 (m, 2H), 7.82−7.09 (m, aromatic and vinyl protons, 11.6H), 4.44−4.19 (m, 2H), 2.19−1.80 (m, 4.8H), 1.47−0.98 (m, 24.0H), 0.94−0.60 (m, 10.0H). IR (KBr): ν [cm^{-1}] 3021, 2977, 2933, 2865, 1596, 1466, 1358, 960 (*trans*-HC═CH), 820. **P6**: yield 76%, green powder. Anal. Calcd: C, 87.77; H, 8.79; N, 3.44. Found: C, 85.22; H, 9.13; N, 3.56). ^{1}H NMR (400 MHz, $CDCl_3$): δ 8.50−8.17 (m, 2H), 7.83−7.09 (m, aromatic and vinyl protons, 10.0H), 4.44−4.19 (m, 2H), 2.19−1.80 (m, 3.0H), 1.47−0.98 (m, 15.0H), 0.94−0.60 (m, 5.5H). IR (KBr): ν [cm^{-1}] 3022, 2976, 2930, 2865, 1596, 1467, 1352, 959 (*trans*-HC═CH), 816.

Poly(9,9-dioctyl-2,7-fluorenylenevinylene-co-2,7-fluoren-9-onylenevinylene) (PFLUOV). A solution of 2,7-dibromo-9,9-dioctylfluorene (0.493 g, 0.90 mmol), 2,7-dibromofluoren-9-one (0.034 g, 0.10 mmol), potassium vinyl trifluoroborate (0.147 g, 1.10 mmol), $Pd(AcO)_2$ (11.0 mg, 0.05 mmol), P(*o*-Tol)$_3$ (0.076 g, 0.25 mmol), triethylamine (0.35 mL, 2.5 mmol) in dioxane (5 mL) was refluxed for 1 day. After cooling to room temperature, the solution was poured into methanol (100 mL). The obtained solid was filtered and dissolved in the minimum amount of chloroform for reprecipitation in methanol. Then, the polymer was washed in a Soxhlet apparatus with acetone and extracted with chloroform to obtain **PFLUOV** in 58% yield as a dark-red solid. M_n = 11 000 Da, M_w = 26 000 Da, D = 2.3. ^{1}H NMR (400 MHz, $CDCl_3$): δ 7.94−7.13 (m, arom and vinyl protons, 8.8H), 2.19−1.80 (m, 4H), 1.47−0.98 (m, 20H), 0.94−0.60 (m, 10H). IR (KBr): ν [cm^{-1}] 3027, 2921, 2852, 1721 (C═O), 1598, 1352, 958 (*trans*-HC═CH), 820.

Poly(9,9-dioctylfluorene) (POF). A 100 mL three necked bottom flask was charged with 2,7-dibromo-9,9-dioctylfluorene (0.548 g, 1.00 mmol), $Ni(COD)_2$ (0.660 g, 2.40 mmol), 2,2′-bipyridine (0.376 g, 2.40 mmol), COD (0.271 g, 2.40 mmol) and toluene (15 mL). The solution was stirred for 4 days at 80 °C. After cooling of the solution, the reaction mixture was diluted with chloroform and treated with a 4 N HCl solution in an extractor funnel until discoloration. The mixture was then washed with a saturated aqueous EDTA solution, a saturated aqueous $NaHCO_3$ solution and brine. The mixture was concentrated and poured into methanol. The solid obtained was filtered and washed with methanol. The product was purified by repeated precipitations in methanol to give **POF** in 46% yield as pale yellow powder. M_n = 24 000 Da, M_w = 67 000 Da. ^{1}H NMR (400 MHz, $CDCl_3$): δ 7.90−7.61 (m, 6H, arom), 2.24−2.00 (m, 4H), 1.29−1.07 (m, 20H), 0.91−0.77 (m, 10H)

Results and Discussion

Polymer Syntheses and Characterization. Chart 1 shows the chemical structure and the preparation of the PFV. The obtainment of **P1**−**P6** was carried out in one-pot starting from 2,7-dibromo-9,9-dioctylfluorene and 3,6-dibromo-*N*-octylcarbazole in the suitable molar ratio with potassium vinyltrifluoroborate, palladium acetate, tri(*o*-tolyl)phosphane and triethylamine in dioxane at reflux. The polymers **P1**−**P6** were obtained in 76−92% yield as green powders. GPC analyses revealed that the number-average molecular weights (6000−11000 Da) of the polymers (Table 1) are similar to those reported in the literature for PFVs obtained by Heck reaction.[9]

The structure of the polymers was confirmed by ^{1}H NMR and FT-IR spectroscopy. ^{1}H NMR analysis was used to assess the copolymer composition by comparison of the C_α proton integrals of the carbazole alkyl chain at ca. 4.20 ppm with the C_α proton integrals of the fluorene alkyl chain and C_β of the carbazole alkyl chain, falling superimposedly at ca. 2.00 ppm (Figure 1). The presence of 1,1-diarylenevinylene defects in the polymers, which can form after the Heck reaction step, was evidenced by the appearance of ^{1}H NMR signals at 5.5−5.6 ppm.[13] The amount of such defects was estimated to be lesser than 10% in all the polymers.

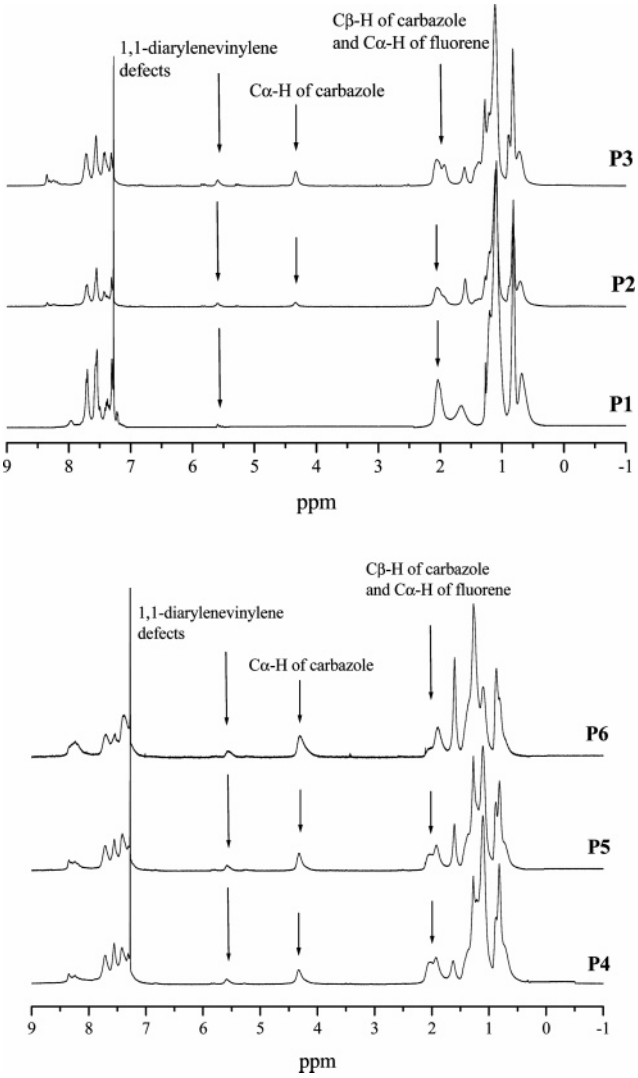

Figure 1. ^{1}H NMR of **P1**−**P6** in $CDCl_3$.

Table 1. Yields, Molecular Weights, and Thermal Properties (Glass Transition Temperatures and Decomposition Temperature at 5% Weight Loss) for P1−P6

polymer	yield (%)	M_n (Da)	M_w (Da)	D	T_g (°C)	T_d (°C)
P1	80	8000	20 000	2.7	56	338
P2	79	11 000	25 000	2.2	55	388
P3	87	7000	14 000	2.0	66	400
P4	91	6000	12 000	2.0	102	388
P5	92	8000	14 000	1.8	101	395
P6	76	6000	10 000	1.7	121	380

The presence of the vinylene functionality was confirmed by the appearance of medium FT-IR bands attributable to the out-of-plane C−H bending of *trans*-vinylene at 957−963 cm^{-1}. The corresponding ^{1}H NMR signals fall in the region of aromatic protons and could not be assigned.

The thermal properties of the polymers were evaluated by means of thermogravimetric analyses (TGA) and differential scanning calorimetry (DSC). A very good thermal stability was revealed for **P1**−**P6**, the weight loss of the polymers being less than 5% below 338 °C (Table 1). The thermal behavior below the decomposition temperature was investigated by DSC that permitted the determination of the glass transition temperature

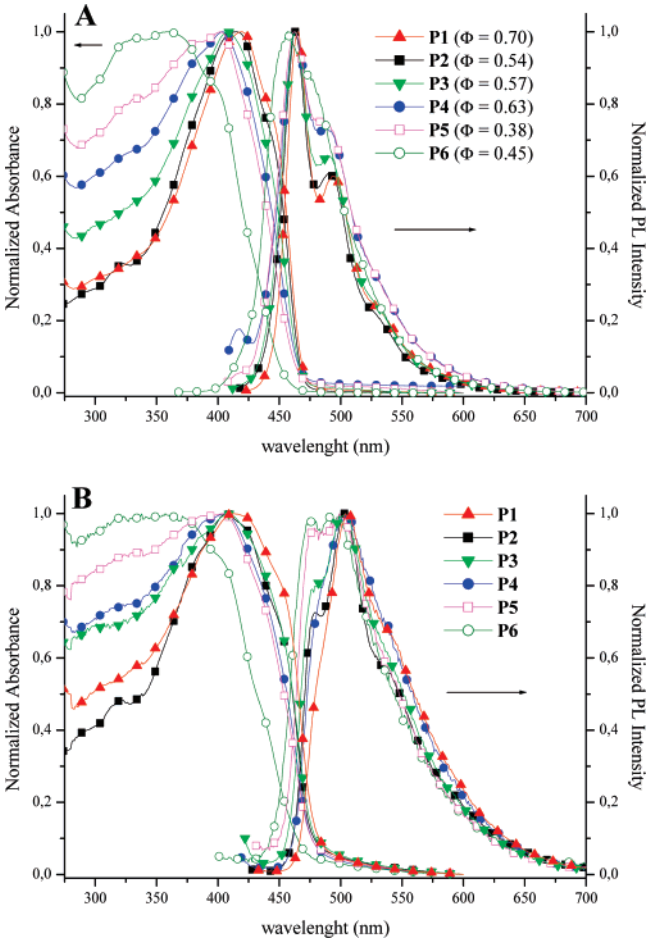

Figure 2. Absorption and PL spectra of **P1**−**P6** recorded in chloroform (A) and as a thin film (B).

(T_g) of the polymers. For **P1**−**3** (carbazole amount 0−40%) thermal events in the range 55−66 °C were observed during the heating scans and could be attributed to glass transitions. As the amount of carbazole in the polymer increased above 40% (in the cases of **P4**−**6**), a considerable raise in T_g was observed. The glass transition events were detected at 101−121 °C. This T_g enhancement can be justified by a decrease of the number of flexible alkyl chains in the polymer, as the carbazole amount increases.

Optical Properties. UV−vis absorption and photoluminescence (PL) features of the polymers in chloroform solution are shown in Figure 2A. Their UV−vis spectra reveal a progressive blue shift of the absorption maxima (from 420 to 361 nm) passing from **P1** to **P6**. The blue-shift of the absorption maxima of the copolymers is correlated with the increasing amount of carbazole that reduces the average π-conjugation extension. This result can be rationalized by considering the random primary structure of the polydispersed materials, which can be seen as a distribution of fluorenylene−vinylene segments of different length spaced by the 3,6-carbazole units, interrupting the π-conjugation extension.

On the other hand, the energy band gaps for **P2**−**P5** (2.60−2.63 eV), which were calculated by the onsets of the absorption curves, are similar to that of **P1** (2.60 eV). Only in the case of **P6**, the high amount of carbazole comonomer causes a distinct increase of the energy band gap to 2.70 eV. These results indicate that the comparable values of the energy band gap in the copolymers are determined by the formation of fluorenylene−vinylene segments of similar extension.

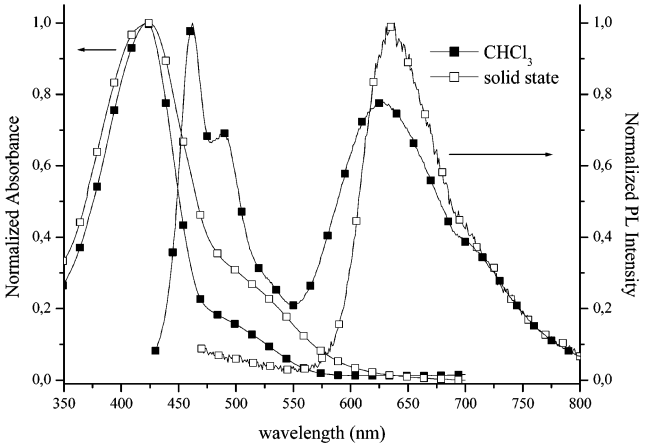

Figure 3. UV−vis and PL spectra of **PFLUOV** in solution and in the solid state.

The emission properties of **P1** (λ_{em} = 464 nm with a vibronic replica at 492 nm) are very similar to those reported for a defect-free PFV prepared by a Horner−Emmons reaction.[18] The fluorescence spectra of **P2**−**P6** are almost identical to that of **P1** because of a fast energy transfer toward the lower energy fluorenylene−vinylene segments. Quantum yields (Φ) were measured in chloroform solutions using 9,10-diphenylanthracene as standard (Φ = 0.90 in cyclohexane)[19] and were comprised in the range $0.38 \leq \Phi \leq 0.70$.

Figure 2B shows the optical properties of the polymers as thin films on quartz. Although the absorption features do not exhibit substantial changes, the fluorescence emission maxima of the materials evidenced a red-shift (475−504 nm), with respect to those obtained in solution, due to conformational changes or interchain interactions in the solid state. The differences of the emission maxima in **P5**−**P6** with respect to **P1**−**P4** are a consequence of an exchange in relative intensity of the vibronic peaks (falling at the same wavelength for all polymers).

Spectral Stability of the Polymers. As it is widely accepted that π-conjugated systems based on 9,9-dialkylfluorene moieties are prone to aerobic oxidation to fluorenones, we deemed it worthwhile to carry out spectral stability test on PFVs by submitting a thin film of **P1** on quartz to a thermal annealing under air and comparing its emission behavior during the thermal stress to that exhibited by poly(9,9-dioctylfluorene) (**POF**). This is a classic procedure for a first stage evaluation of the spectral stability of emitting materials and has been widely applied for investigating the causes of the appearance of the green emission band in PFs, proving the direct correlation between fluorene oxidation to fluorenone and appearance of the low-energy band.[6] In the framework of our studies, we first report on the spectral behavior of PFVs. Preliminarily, the effect of the presence of fluorenone units in a PFV structure on its optical properties was investigated by preparing **PFLUOV** by the Suzuki−Heck cascade polymerization between potassium vinyltrifluoroborate, 2,7-dibromodioctylfluorene, and 2,7-dibromofluorenone (10% mol/mol with respect to dioctylfluorene, Chart 1). Figure 3 shows the absorption and emission properties of **PFLUOV** in solution and in the solid state.

As evident in Figure 3, both in solution and in the solid state, the absorption spectrum of **PFLUOV** shows a maximum at 423 nm, due to the fluorenylene−vinylene backbone, along with a tail at longer wavelength caused by the π−π* charge transfer absorption due to the fluorenone chromophore. In the photoluminescence spectrum recorded in chloroform, along with the band at 465 nm ascribable to the PFV backbone emission, a

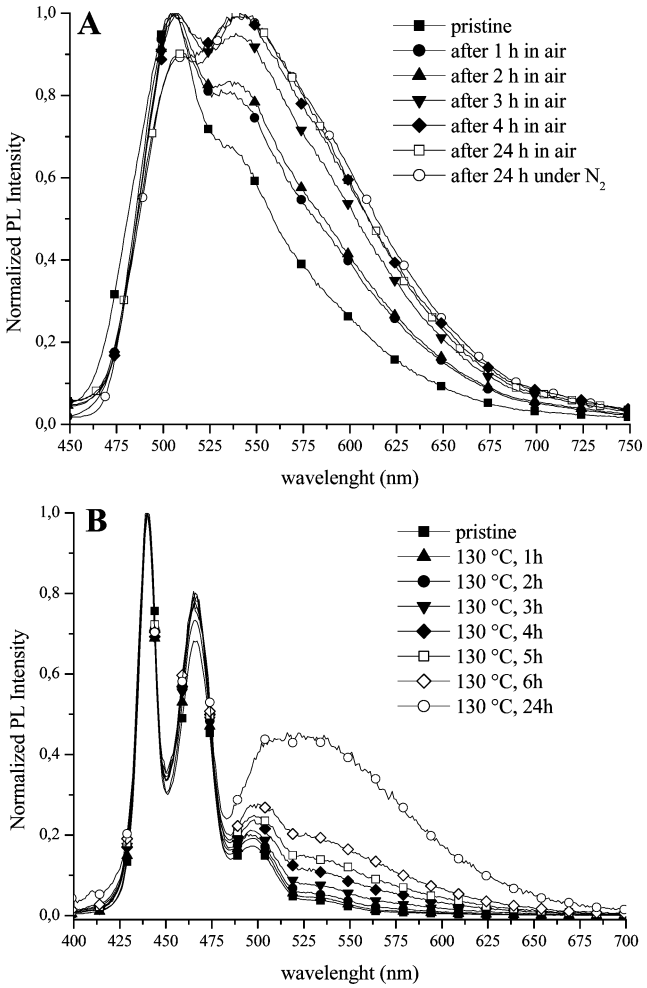

Figure 4. PL spectra of **P1** (A, λ_{ex} = 400 nm) and **POF** (B, λ_{ex} = 380 nm) in the solid state during a thermal annealing in air at 130 °C.

band at 635 nm appears, caused by the presence of the fluorenone comonomer. In the solid state, a complete quenching of the blue-green emission component was observed.

As to the question of the physical origin of this low-energy emission,[6,7] the optical behavior of **PFLUOV** can be interpreted both by fluorenone-based excimers or on-chain fluorenone emission. However, the presence of a shoulder in the red-emission of **PFLUOV** seems to indicate that the origin of such band is related to the charge-transfer $\pi-\pi^*$ transition, deriving from the presence of the carbonyl group, and not to fluorenone-based excimers, the emission of which generally appears as a featureless broad band. The on-chain fluorenone emission can be seen as a consequence of an efficient energy transfer from the fluorenylene−vinylene segments to fluorenone acceptors. This hypothesis is strongly corroborated by the fact that the PFV backbone emission overlaps the fluorenone charge-transfer $\pi-\pi^*$ transition absorption (Figure 3). The energy transfer toward fluorenone moieties, more efficient in the solid state, can satisfactorily explain the optical behavior of **PFLUOV** as thin film.

Next, we studied the optical behavior of **P1** during thermal annealing in the solid state under air at 130 °C. The evolution of the photoluminescence properties of **P1** during thermal annealing is shown in Figure 4A. On the basis of the results carried out on **PFLUOV**, we expected the appearance of a band located at 635 nm in the PL spectrum of **P1**, in the case of fluorenone formation during the thermal stress. However, only a variation of the intensity of the vibronic peak at about 550 nm was observed. Noteworthy, the same effect was observed submitting the polymer film to a thermal annealing under nitrogen atmosphere. This is a very clear indication that the emission profile change in the course of the thermal annealing under air cannot be attributed to oxidative degradation due to fluorenone formation, but presumably to conformational rearrangements. Carrying out the same thermal annealing on **POF** causes, on the other hand, the well-known appearance of a green emission band induced by fluorenone formation (Figure 4B).

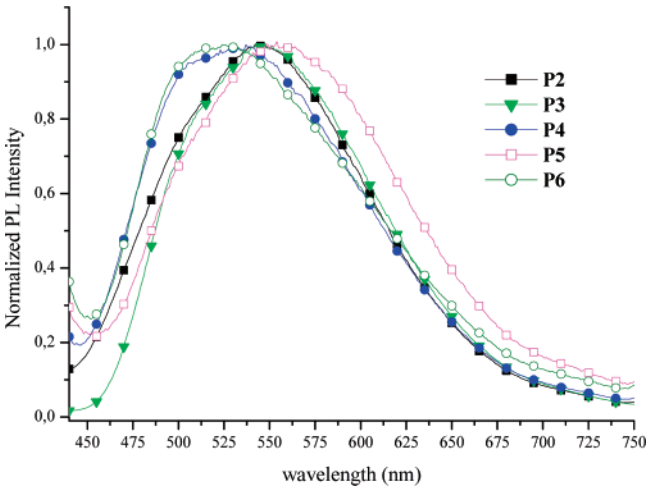

Figure 5. PL spectra (λ_{ex} = 400 nm) of **P2**−**P6** after thermal annealing at 130 °C in air.

Notwithstanding the two polymers derive from the same batch of fluorene monomers, the differences in their spectral stability are remarkable. Recently, it has been claimed that the degradation of fluorene-based materials is to be ascribed to radical processes,[20] as confirmed by the formation of an insoluble residue after thermal annealing due to the recombination of nearby radicals. After 24 h thermal stress on **POF**, in fact, the almost complete insolubility of the polymer film in common organic solvents could be noted. In the case of **P1**, on the contrary, the residue film after 24 h of thermal annealing was completely soluble in chloroform. On the basis of these results, it can be stated that, once formed in **P1**, radicals preferentially react with the backbone double bonds, which act as radical traps. The explanation of this behavior may reside in the fact that, for steric reasons, recombination between radicals located on the polymer backbone is less probable than that between radicals located on the side alkyl chain.[21] Therefore, although it is reasonable to suppose that the degradation of **P1** occurs in any case, it can safely be assumed that this process involves vinylene moieties, leaving the fluorene C-9 position intact, thus preserving its emission properties under thermal oxidation. However, an oxidative degradation of vinylene moieties in **P1** (that would cause the expected emission blue shift as reported for PAVs[22]) seems to be inhibited by the steric shield of the π-conjugated backbone provided by the alkyl chains.

The same oxidative treatment (130 °C in air) was carried out on **P2**−**P6** films as shown in Figure 5, revealing that also these polymers must be optically stable, as no band at 635 nm ascribable to fluorenone emission was evidenced.

Electrochemical Behavior of P1−**P6.** The knowledge of the HOMO and LUMO energy levels of π-conjugated materials is crucial for the comprehension and optimization of OLED performances. Cyclic voltammetry (CV) is a well-established method for the evaluation of the ionization potential and of the electron affinity of a material, from which, by following the empirical relationships proposed by de Leeuw et al.,[23] it is

Table 2. Electrochemical Properties of P1−P6

	electrochemical properties				OLED characteristics			
polymer	$E_{onset,ox}$ (V)[a]	HOMO (eV)	energy gap (eV)[b]	LUMO (eV)	max lumin (cd/m^2)	max curr eff (cd/A)	max ext eff (%)	CIE[c] (*x*,*y*)
P1	0.600	−5.40	2.60	−2.80	20	0.0015	0.0006	0.24; 0.37
P2	0.695	−5.49	2.60	−2.89	150	0.0075	0.003	0.32; 0.35
P3	0.562	−5.36	2.62	−2.74	190	0.0073	0.003	0.29; 0.43
P4	0.602	−5.40	2.62	−2.78	100	0.0045	0.002	0.27; 0.40
P5	0.818	−5.62	2.63	−2.99	450	0.0225	0.01	0.23; 0.36
P6	0.845	−5.64	2.70	−2.93	40	0.0025	0.001	0.28; 0.38

[a] Onset of oxidation potentials. [b] Estimated from the onset of absorption in the UV−vis spectrum) and features of OLED devices. [c] CIE coordinates obtained from spectra at 14 V.

possible to obtain the HOMO and LUMO energy levels. Although HOMO energy values calculated by CV may not be extremely accurate, this technique is especially useful for the comparison of ionization potential of polymers with similar structures.

CV measurements were performed on an indium−tin oxide (ITO) electrode coated with a thin film of the relevant polymer. These conditions simulate the situation of hole injection in OLEDs, as ITO is commonly used as transparent anode. For **P1**−**P6**, only irreversible oxidation waves could be recorded, revealing rather unstable hole-charged states of the polymers. As expected, no reduction wave was observed for any of the polymer probably because of the interfacial energy barrier for the electron injection. The HOMO energy levels of **P1**−**P6**, reported in Table 2, were calculated from the onset of oxidation waves. These values for **P1**−**P4** (ranging between −5.36 and −5.49 eV) do not exhibit substantial differences.

This behavior is to be related to the simultaneous presence of two effects ascribable to the amount of the carbazole comonomer on the HOMO energy level: the electron-donor properties of carbazole nitrogen atoms and the π-conjugation extension. It has to be supposed that the expected increase in the HOMO energy level upon increase of the carbazole amount in the polymer (due to inductive effects) is counterbalanced by the lowering of the π-conjugation extension (due to the 3,6-carbazole linkage).[24] Combining the electrochemical data with the UV−vis absorption onset allows an estimate of the LUMO energy levels. As the energy gap of **P1**−**P4** (2.60−2.62 eV) and the HOMO levels do not remarkably change, their LUMO energy levels are consequently very similar (in the range −2.74 to −2.89 eV).

On the contrary, the high amount of carbazole in **P5** and **P6** lowers the average π-conjugation extension and, consequently, their HOMO energy levels to −5.62 and −5.64 eV respectively. As a consequence of an almost unaltered edge of their UV−vis absorption spectra (2.63 and 2.70 eV for **P5** and **P6** respectively), a better electron affinity of these polymers can be deduced (−2.99 and −2.93 eV for **P5** and **P6** respectively).

Electroluminescence Properties. In order to investigate the electroluminescence performances of the synthesized polymers, diodes of ITO/PEDOT−PSS/polymer/Ca/Al configuration were fabricated and measured in air, also aiming at evaluating their spectral stability. The diodes exhibit a bluish-green light emission and turn-on voltages of about 10−12 V. These high values can be a consequence of the poor electron injection at the interface between the polymer and the calcium cathode, as anticipated by their electrochemistry in the reduction scans (vide supra). In the case of **P1**, the turn-on voltage of 12 V was found to be higher than those of a similar polymer obtained by the Gilch reaction[10a] and the reasons of this behavior could be ascribed to the presence of metal residues[25] deriving from the polymerization procedure. However, our results are compatible with turn-on voltages (about 15 V) reported for devices based on polymers structurally similar to **P1** but obtained by Heck reaction.[9]

The comparison between the maximum luminance (cd/m^2) and maximum current efficiencies (cd/A) of the polymers (Table 2) indicates that the incorporation of carbazole in **P2**−**P4** determines an improvement of the device performance with respect to **P1** (20 cd/m^2 at 18 V). Although mobility measurements were not carried out on the polymers, this observation can be explained by the better hole transport in **P2**−**P4** deriving from the presence of carbazole moieties,[26] with their HOMO and LUMO energy levels being very similar. This explanation is corroborated by the evident increase of the current density of **P2**−**P4** with respect to **P1** at the same voltages (Figure 6). However, it can reasonably be supposed that in these polymers, once injected, most of the holes move rapidly toward the cathode without exciton formation by recombination with electrons. This partly justifies the relatively low performances of **P2**−**P4** in our unoptimized LEDs.

On the other hand, acceptable LED performances (450 cd/m^2, 0.0225 cd/A) were achieved in the case of **P5**. Since the introduction of holes in the diodes cannot be considered the limiting step for the performance of the devices (because of the presence of the PEDOT−PSS layer), the higher current effciences of **P5** can be seen as a consequence of its higher electron affinity (as indicated by its lower LUMO energy level) favoring the electron injection in the active layer of the device. The external efficiency of the device based on **P5** was 0.010% and, as expected, was remarkably higher than that obtained for the others. Notwithstanding the electron affinity similar to that of **P5**, **P6** exhibited poor performance in electroluminescence. The reasons of this behavior and the analysis of the electroluminescence profiles of the polymers (reported in Figure 7) deserves a detailed explanation.

Differently from **P1**, which exhibits a well-defined vibronic structrure in emission, the other polymers show a quite broad emission band. Because of the similarity of the glass transition temperatures of the polymers, this behavior cannot be justified by aggregation and/or conformational changes in the solid state, consequence of the temperatures reached in devices. A plausible explanation for the broadness of the electroluminescence spectra of **P2**−**P6** could be the fluorenone formation during LED operation. Notwithstanding that the polymers derive from the same batch of 2,7-dibromo-9,9-dioctylfluorene, the appearance of the fluorenone emission band at 635 nm is evident passing from **P2** to **P6**, probably because the higher tendency to strong intermolecular interactions leads to a more efficient energy transfer from the 9,9-dioctylfluorenylene−vinylene segments toward the emitting fluorenone defects (an acknowledged pathway for fluorenone emission in polyfluorene systems[6]). In our PFVs, the molecular interactions between adjacent polymer chains are enhanced with the increasing amount of carbazole

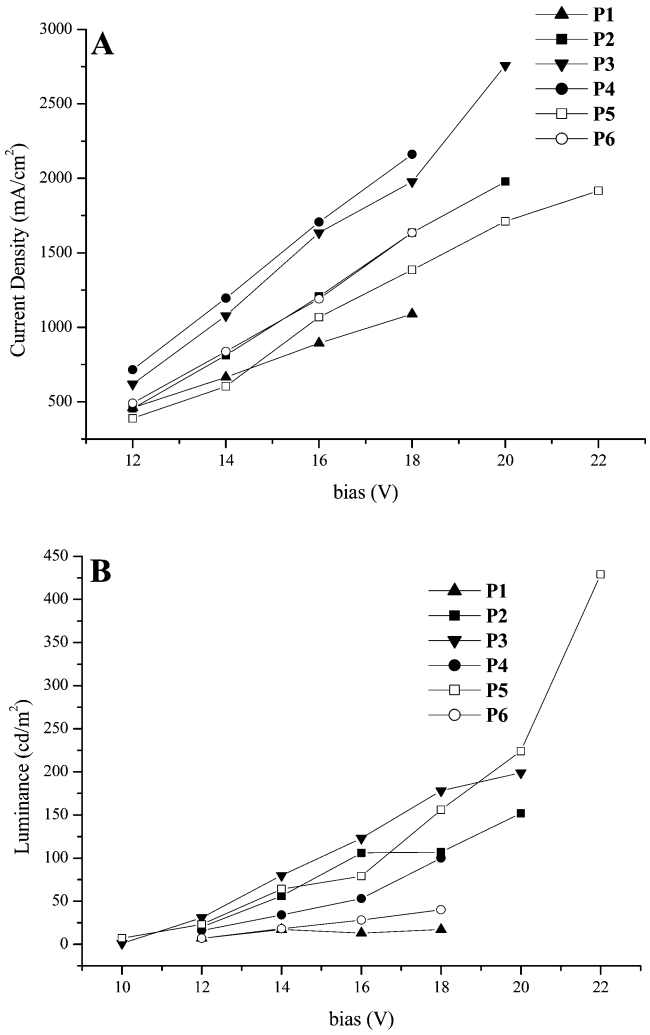

Figure 6. Current density (A) and luminance (B) plots of the ITO/PEDOT−PSS/**P1**−**P6**/Ca/Al diodes.

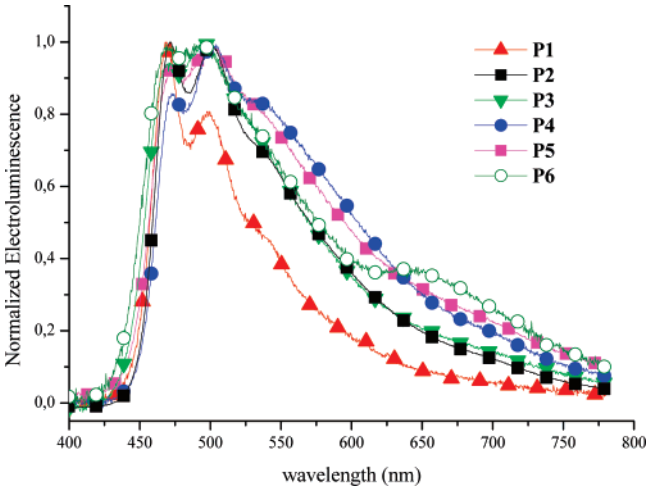

Figure 7. EL spectra of the ITO/PEDOT−PSS/**P1**−**P6**/Ca/Al diodes at 16 V.

because of the decrease in the number of fluorene dialkyl groups, the role of which is to keep different π-systems from interacting with each other. For these reasons, the fluorenone emission at 635 nm is more evident in **P6**. The low performances of this polymer in the device can consequently be ascribed to its higher amount of carbazole maximizing local interchain interactions, that induce nonradiative decay pathways for excitons, and an efficient energy transfer toward fluorenone defects.

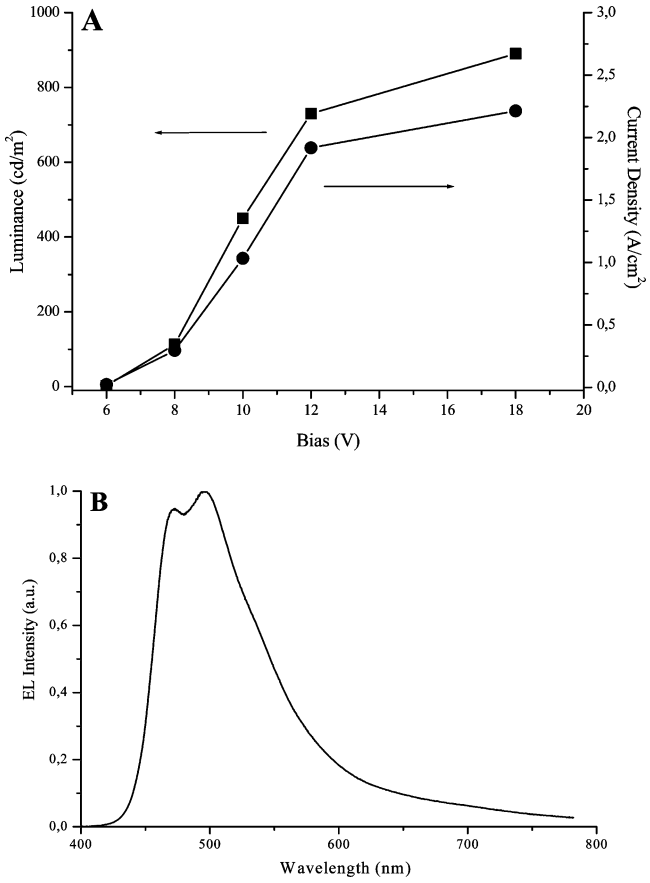

Figure 8. Current density and luminance plots of the ITO/PEDOT−PSS/**P5**/Alq_3/Ca/Al diode (A) and its electroluminescence spectrum at 12 V (B).

Eventually, in order to optimize the performances, we chose to construct a device based on **P5** and preventing the electron injection problems by deposition of 5 nm of aluminum(III) tris-(8-hydroxyquinolinate) (Alq_3) between the polymer and the calcium cathode, which functioned as electron injection layer. The configuration ITO/PEDOT−PSS/**P5**/Alq_3/Ca/Al of the diode, improved considerably the device performances (Figure 8). First, the turn on voltage of the optimized OLED was lowered to 6 V. Then, the maximum luminance (890 cd/m^2) was remarkably improved with respect to the unoptimized device (450 cd/m^2) and was obtained at a much lower voltage (18V). The maximum external efficiency (0.017%) and the maximum current efficiency (0.0435 cd/A at 10V) were almost doubled. Finally, the electroluminescence spectrum (CIE coordinates: $x = 0.22$; $y = 0.36$ at 14 V) was not altered by the introduction of the electron injecting layer.

Conclusions

The synthesis of poly(9,9-dioctyl-2,7-fluorenylenevinylene) (**P1**) and a series of new random poly(9,9-dioctyl-2,7-fluorenylenevinylene-*co*-*N*-octyl-3,6-carbazolylenevinylene) copolymers (at 20−80% mol/mol of carbazole, **P2**−**P6**) was achieved by the Suzuki−Heck cascade reaction. The polymers were obtained in good yields and exhibited moderate molecular weights. Very good thermal stability and glass transition temperatures dependent on the copolymer composition (in the range between 55 and 125 °C) were deduced by thermal analysis. Differently from the PL emission of the copolymers, which were found to be similar both in solution and in the solid state, their UV−vis features evidenced a slight blue shift of the absorption maxima as a function of the carbazole amount, due

to the interruption of the π-conjugation extension caused by the 3,6-linkage at the carbazole moiety. The control of such aspect permitted the tuning of the HOMO and LUMO energy levels, as demonstrated by CV measurements, without remarkably changing the emission properties of the materials.

Moreover, since fluorene-based polymers are prone to fluorenone formation, an investigation was performed on the photoluminescence spectral stability of **P1** under aerobic thermal annealing. The results evidenced a remarkably higher spectral stability with respect to **POF**, presumably because of the preferential oxidation of vinylene functionality with respect to the fluorene C-9 position. The absence of fluorenone formation in **P1** under thermal stress was confirmed by comparison with the photoluminescence features exhibited by a PFV containing fluorenone (10% mol/mol) as comonomer.

The electroluminescence properties of the polymers were tested by constructing suitable OLED devices of configuration ITO/PEDOT−PSS/(**P1**−**P6**)/Ca/Al. It was proven that the incorporation of carbazole in **P2**−**P4** determines an improvement of the device performance with respect to **P1**. This result can be rationalized in terms of the better hole transport in the material due to the presence of carbazole moieties. The best performances (450 cd/m^2, 0.0225 cd/A at 22 V, 0.010% ext. eff.) were obtained for the OLEDs based on **P5** (60% mol/mol carbazole), due to the higher LUMO energy level (−2.99 eV) that favors the injection and transport of electrons in the device respect to the other materials. These figures of merit could be improved by inserting an electron injecting layer (Alq_3) between the cathode and the polymer (890 cd/m^2, 0.0435 at 10 V, 0.017% ext eff). These results pave the way for future studies on the optimization of HOMO−LUMO energy level of a π-conjugated arylene−vinylene copolymer by control of its composition, in particular with our Suzuki−Heck cascade method, that allows the obtainment of random copolymers unobtainable with the classic synthetic procedures.

Acknowledgment. The FIRB project MICROPOLYS (Italian MIUR) is gratefully acknowledged for funding.

Supporting Information Available: Figures giving TGA and DSC and cyclic voltammetry scans for **P1**−**P6**. This material is available free of charge via the Internet at http://pubs.acs.org.

References and Notes

(1) Burroughes, J. H.; Bradley, D. D. C.; Brown, A. R.; Marks, R. N.; Mackay, K.; Friend, R. H.; Burns, P. L.; Holmes, A. B. *Nature (London)* **1990**, *347*, 539−541.

(2) Seki, K.; Furuyama, T.; Kawasumi, T.; Sakurai, Y.; Ishii, H.; Kajikawa, K.; Ouchi, Y.; Masuda, T. *J. Phys. Chem. B* **1997**, *101*, 9165−9169.

(3) (a) Bernius, M. T.; Inbasekaran, M.; O'Brien, J.; Wu, W. *Adv. Mater.* **2000**, *12*, 1737−1750. (b) Mitschke, U.; Bäuerle, P *J. Mater. Chem.* **2000**, *10*, 1471−1507. (c) Kraft, A.; Grimsdale, A. C.; Holmes, A. B. *Angew. Chem., Int. Ed.* **1998**, *37*, 402−428.

(4) (a) Scherf, U.; List, E. J. W. *Adv. Mater.* **2002**, *14*, 477−487. (b) Neher, D. *Macromol. Rapid Commun.* **2001**, *22*, 1365−1385.

(5) (a) Gaal, M.; List, E. J. W.; Scherf, U. *Macromolecules* **2003**, *36*, 4236−4237. (b) List, E. J. W.; Guenter, R.; Scandiucci de Freitas, P.; Scherf, U. *Adv. Mater.* **2002**, *14*, 374−378. (c) Bliznyuk, V. N.; Carter, S. A.; Scott, J. C.; Klärner, G.; Miller, R. D.; Miller, D. C. *Macromolecules* **1999**, *32*, 361−369. (d) Lee, J.-I.; Klärner, G.; Miller, R. D. *Chem. Mater.* **1999**, *11*, 1083−1088.

(6) (a) Becker, K.; Lupton, J. M.; Feldmann, J.; Nehls, B. S.; Galbrecht, F.; Gao, D.; Scherf, U. *Adv. Funct. Mater.* **2006**, *16*, 364−370. (b) Chi, C.; Im, C.; Enkelmann, V.; Ziegler, A.; Lieser, G.; Wegner, G. *Chem.−Eur. J.* **2005**, *11*, 6833−6845. (c) Li, J.; Li, M.; Bo, Z. *Chem.−Eur. J.* **2005**, *11*, 6930−6936. (d) Kulkarni, A. P.; Kong, X.; Jenekhe, S. A. *J. Phys. Chem. B* **2004**, *108*, 8689−8701. (e) Romaner, L.; Pogantsch, A.; Scandiucci de Freitas, P.; Scherf, U.; Gaal, M.; Zojer, E.; List, E. J. W. *Adv. Funct. Mater.* **2003**, *13*, 597−601. (f) Zojer, E.; Pogantsch, A.; Hennebicq, E.; Beljonne, D.; Brédas, J.-L.; Scandiucci de Freitas, P.; Scherf, U.; List, E. J. W. *J. Chem. Phys.* **2002**, *117*, 6794−6802.

(7) (a) Yang, G.-Z.; Wu, M.; Lu, S.; Wang, M.; Liu, T.; Huang, W. *Polymer* **2006**, *47*, 4816−4823. (b) Jaramillo-Isaza, F.; Turner, M. L. *J. Mater. Chem.* **2006**, *16*, 83−89. (c) Sims, M.; Bradley, D. D. C.; Ariu, M.; Koeberg, M.; Asimakis, A.; Grell, M.; Lidzey, D. G. *Adv. Funct. Mater.* **2004**, *14*, 765−781.

(8) (a) Ahn, T.; Song, S.-Y.; Shim, H.-K. *Macromolecules* **2000**, *33*, 6764−6771. (b) Kim, J. K.; Yu, J. W.; Hong, J. M.; Cho, H. N.; Kim, D. Y.; Kim, C. Y. *J. Mater. Chem.* **1999**, *9*, 2171−2176. (c) Kim, J. K.; Hong, S. I.; Cho, H. N.; Kim, D. Y.; Kim, C. Y. *Polym. Bull. (Berlin)* **1997**, *38*, 169−176.

(9) Mikroyannidis, J. A.; Yu, Y.-J.; Lee, S.-H.; Jin, J.-I. *J. Polym. Sci., Part A: Polym. Chem.* **2006**, *44*, 4494−4507.

(10) (a) Jin, S. H.; Kang, S. Y.; Kim, M. Y.; Chan, Y. U.; Kim, J. Y.; Lee, K.; Gal, Y. S. *Macromolecules* **2003**, *36*, 3841−3847. (b) Jin, S. H.; Park, H. J.; Kim, J. Y.; Lee, K.; Lee, S. P.; Moon, D. K.; Lee, H. J.; Gal, Y. S. *Macromolecules* **2002**, *35*, 7532−7534.

(11) Taranekar, P.; Abdulbaki, M.; Krishnamoorti, R.; Phanichphant, S.; Waenkaew, P.; Patton, D.; Fulghum, T.; Advincula, R. *Macromolecules* **2006**, *39*, 3848−3854.

(12) Shin, W. S.; Joo, M.-K.; Kim, S. C.; Park, S.-M.; Jin, S.-H.; Shim, J.-M.; Lee, J. K.; Lee, J. W.; Gal, Y.-S.; Jenekhe, S. A. *J. Mater. Chem.* **2006**, *16*, 4123−4132.

(13) Grisorio, R.; Mastrorilli, P.; Nobile, C. F.; Romanazzi, G.; Suranna, G. P. *Tetrahedron Lett.* **2005**, *46*, 2555−2558.

(14) Becker, H.; Spreitzer, H.; Kreuder, W.; Kluge, E.; Schenk, H.; Parker, I.; Cao, Y. *Adv. Mater.* **2000**, *12*, 42−48.

(15) (a) Morin, J.-F.; Leclerc, M.; Adès, D.; Siove, A. *Macromol. Rapid Commun.* **2005**, *26*, 761−778. (b) Chen, Y.; Hwang, S.-W.; Chen, S.-H. *J. Polym. Sci., Part B: Polym. Phys.* **2004**, *42*, 333−340. (c) Li, H.; Zhang, Y.; Hu, Y.; Ma, D.; Wang, L.; Jing, X.; Wang, F. *Macromol. Chem. Phys.* **2004**, *205*, 247−255. (d) Chen, S.-H.; Hwang, S.-W.; Chen, Y. *J. Polym. Sci., Part A: Polym. Chem.* **2004**, *42*, 883−893. (e) Kim, J. J.; Kim, K.-S.; Baek, S.; Kim, H. C.; Ree, M. *J. Polym. Sci., Part A: Polym. Chem.* **2002**, *40*, 1173−1183. (f) Paik, K. L.; Baek, N. S.; Kim, H. K.; Lee, J.-H.; Lee, Y. *Macromolecules* **2002**, *35*, 6782−6791. (g) Ahn, T.; Shim, H.-K. *Macromol. Chem. Phys.* **2001**, *202*, 3180−3188. (h) Meng, H.; Chen, Z.-K.; Huang, W. *J. Phys. Chem. B* **1999**, *103*, 6429−6433. (i) Song, S.-Y.; Jang, M. S.; Shim, H.-K.; Hwang, D.-H.; Zyung, T. *Macromolecules* **1999**, *32*, 1482−1487.

(16) Grisorio, R.; Mastrorilli, P.; Nobile, C. F.; Romanazzi, G.; Suranna, G. P.; Acierno, D.; Amendola, E. *Macromol. Chem. Phys.* **2005**, *206*, 448−455.

(17) Molander, G. A.; Rivero, M. R. *Org. Lett.* **2002**, *4*, 107−109.

(18) Anuragudom, P.; Newaz, S. S.; Phanichphant, S.; Lee, T. R. *Macromolecules* **2006**; *39*, 3494−3499.

(19) Demas, J. N.; Crosby, G. A. *J. Phys. Chem.* **1971**, *75*, 991−1024.

(20) (a) Liu, L.; Tang, S.; Liu, M.; Xie, Z.; Zhang, W.; Lu, P.; Hanif, M.; Ma, Y. *J. Phys. Chem. B* **2006**, *110*, 13734−13740. (b) Liu, L.; Qiu, S.; Wang, B.; Zhang, W.; Lu, P.; Xie, Z.; Hanif, M.; Ma, Y.; Shen, J. *J. Phys. Chem. B* **2005**, *109*, 23366−23370. (c) Zhao, W.; Cao, T.; White, J. M. *Adv. Funct. Mater.* **2004**, *14*, 783−790.

(21) Bao, Z.; Chen, Y.; Cai, R.; Yu, L. *Macromolecules* **1993**, *26*, 5281−5286.

(22) Scurlock, R. D.; Wang, B.; Ogilby, P. R.; Sheats, J. R.; Clough, R. L. *J. Am. Chem. Soc.* **1995**, *117*, 10194−10202.

(23) De Leeuw, D. M.; Simenon, M. M. J.; Brown, A. R.; Einerhand, R. E. F. *Synth. Met.* **1997**, *87*, 53−59.

(24) Chi, C.; Wegner, G. *Macromol. Rapid Commun.* **2005**, *26*, 1532−1537.

(25) (a) Krebs, F. C.; Nyberg, R. B.; Jorgensen, M. *Chem. Mater.* **2004**, *16*, 1313−1318. (b) Nielsen, K. T.; Bechgaard, K.; Krebs, F. C. *Macromolecules* **2005**, *38*, 658−659.

(26) (a) Lu, J.; Tao, Y.; D'iorio, M.; Li, Y.; Ding, J.; Day, M. *Macromolecules* **2004**, *37*, 2442−2449. (b) Stéphan, O.; Vial, J. C. *Synth. Met.* **1999**, *106*, 115−119.

MA070221Q